Biomaterials 33 (2012) 7556–7564

Contents lists available at SciVerse ScienceDirect

Biomaterials

journal homepage: www.elsevier.com/locate/biomaterials

Self-assembled complex of probe peptide – *E. Coli* RNA I conjugate and nano graphene oxide for apoptosis diagnosis

Won Ho Kong [a,1], Dong Kyung Sung [b,1], Ki Su Kim [a], Ho Sang Jung [a], Eun Ji Gho [a], Seok Hyun Yun [c], Sei Kwang Hahn [a,c,*]

[a] Department of Materials Science and Engineering, Pohang University of Science and Technology (POSTECH), San 31 Hyoja-dong, Nam-gu, Pohang, Kyungbuk 790-784, South Korea
[b] Samsung Biomedical Research Institute, 50 Irwon-dong, Gangnam-Gu, Seoul, 135-710, South Korea
[c] Wellman Center for Photomedicine, Harvard Medical School and Massachusetts General Hospital, 65 Landsdowne St. UP-513, Cambridge, MA 02139, USA

ARTICLE INFO

Article history:
Received 11 June 2012
Accepted 28 June 2012
Available online 20 July 2012

Keywords:
Graphene oxide
Caspase
π-π stacking
Apoptosis
Diagnosis

ABSTRACT

Caspase-3 plays an important role in the initiation and propagation of apoptosis which is involved in various kinds of diseases including neurodegenerative diseases and inflammatory diseases. The capase-3 cleavable site of Asp-Glu-Val-Asp (DEVD) connected to a partial sequence of *Escherichia coli* RNAI was labeled with tetramethyl-6-carboxyrhodamine (TAMRA) as an optical probe. Graphene oxide (GO) was synthesized by a modified Hummer's method and exploited for the preparation of nano-sized GO (NGO) conjugated with polyethylene glycol (PEG). After binding the NGO-PEG by π-π stacking, the quenched fluorescence of TAMRA-DEVD-single stranded DNA (ssDNA) conjugate was recovered via the enzymatic cleavage by caspase-3 in live A549 cells. The comparative study with terminal deoxynucleotidyl transferase dUTP nick end labeling (TUNEL) assay clearly confirmed the specific detection of apoptosis by the non-covalent TAMRA-DEVD-ssDNA/NGO-PEG complex. Furthermore, the self-assembled NGO complex was successfully exploited for *in vivo* diagnosis of apoptosis-related diseases like hypoxic-ischemic encephalopathy (HIE) and liver cirrhosis.

1. Introduction

The progress of diagnosis is highly dependent on the development of nanomaterials that offer a simple, rapid, cost-effective, and *in situ* monitoring platform for biosensing and bioimaging applications [1–5]. Graphene oxide (GO), a special member of carbon nanomaterials family [2,6,7], has a unique physical property to bind biomolecules, such as nucleic acids [8], peptides [9], and aromatic chemical compounds [10,11], by π-π stacking. The complex formation can cause a long range fluorescence resonance energy transfer (FRET) from an attached dye on the biomolecule to graphene resulting in the fluorescence quenching [12]. Accordingly, nano-sized GO (NGO) derivatives have been widely exploited for a variety of biomedical applications. NGO has been investigated for controlled delivery of gene and cancer therapeutics with a high drug loading efficiency on both sides of the graphitic domain [10,11]. NGO can work as a photoabsorber for a photothermal ablation therapy [13]. In addition, NGO based hybrid bionanomaterials have shown a great potential as attractive and powerful tools for biosensing and bioimaging to detect nucleic acids [14], peptides [9], proteins [15], viruses [16], and small molecules [17].

Apoptosis is an important physiological event of cell loss which depends on pre-existing and *de novo* proteins for the highly regulated pathway [18]. Among them, caspase-3 is particularly known to be directly involved in the initiation and propagation of apoptosis [18,19]. Apoptosis is highly related with various kinds of diseases such as neurodegenerative diseases, inflammatory diseases, cancer, autoimmune diseases, and hematologic diseases [18,20–22]. However, the conventional assays for the detection of apoptosis including terminal deoxynucleotidyl transferase dUTP nick end labeling (TUNEL) and Annexin V assays are inefficient and time-consuming due to the nonspecificity and the complicated multiple processes [23]. Despite wide investigations [19,23–26], there are few reports on *in vivo* monitoring of caspase for diagnostic applications.

In this work, taking advantages of π-π stacking between graphene and single stranded DNA (ssDNA), and the fluorescence quenching by FRET, we developed a facile platform of the near-infrared fluorescent (NIRF) probe peptide – ssDNA/polyethylene glycol (PEG) conjugated NGO (NGO-PEG) complex for the diagnosis of apoptosis related diseases. Tetramethyl-6-carboxyrhodamine

* Corresponding author. Tel.: +82 54 279 2159; fax: +82 54 279 2399.
E-mail address: skhanb@postech.ac.kr (S.K. Hahn).
[1] These authors contributed equally to this work.

0142-9612/$ – see front matter © 2012 Elsevier Ltd. All rights reserved.
http://dx.doi.org/10.1016/j.biomaterials.2012.06.086

(TAMRA) labeled capase-3 cleavable site of Asp-Glu-Val-Asp (DEVD) was conjugated to a partial sequence of *Escherichia coli* (*E. coli*) RNAI, which was self-assembled with NGO-PEG to prepare TAMRA-DEVD-ssDNA/NGO-PEG complex. After *in vitro* bioimaging of caspase-3 activity in live cells, the non-covalent TAMRA-DEVD-ssDNA/NGO-PEG complex was exploited and discussed for *in vivo* facile diagnosis of apoptosis-related diseases.

2. Materials and methods

2.1. Materials

Natural graphite powder, sulfuric acid (H_2SO_4), sodium nitrate ($NaNO_3$), potassium permanganate ($KMnO_4$), chloroacetic acid ($ClCH_2COOH$), tumor necrosis factor-related apoptosis-inducing ligand (TRAIL), staurosporine (STS), 4′,6-diamidino-2-phenylindole (DAPI), bovine serum albumin (BSA), caspase-3 and its inhibitor, Z-DEVD-FMK, were purchased from Sigma–Aldrich (St. Louis, MO). 5′-Thiol-modified partial sequence of *E. coli* RNA I (5′-ATC TCG GCT CTG CTA GCG-3′) was purchased from Bioneer (Daejon, Korea). C-terminal amine functionalized fluorescent caspase-3 specific probe peptide (TAMRA-GDEVDAP) was purchased from Peptron (Daejon, Korea). 1-Ethyl-3-[3-(dimethylamino)propyl]carbodiimide (EDC) and N-(E-malemidocaproyloxy)sulfo-succinimide (Sulfo-EMCS) were purchased from Pierce (Rockford, IL). Hydrogen peroxide (H_2O_2) was purchased from Junsei Chemical (Tokyo, Japan) and polyethylene glycol (PEG) was purchased from Sunbio (Seoul, Korea). All reagents were used without further purification.

2.2. Synthesis of fluorescently labeled capase-3 specific probe

To prepare fluorescently labeled caspase-3 specific probe, 50 nmol of NIRF TAMRA-labeled DEVD peptide (f-DEVD) with a free amino group at C-terminal was reacted with 50 nmol of sulfo-EMCS in PBS (pH = 7.2). After vigorous stirring at room temperature for 1 h, the resulting maleimide-functionalized f-DEVD peptide was reacted with 0.9 equimolar amount of 5′-sulfhydryl-modified ssDNA for 6 h with mild stirring. The remaining cross-linker and unreacted peptide fragment were eliminated using a dextran desalting column (MWCO = 5 K), and further purified by dialysis (MWCO = 10 K) against deionized water. The resulting products were collected, concentrated using a SpeedVac evaporator (Thermo, Madison, WI), and analyzed by 2% agarose gel electrophoresis in ×0.5 TBE buffer and gel permeation chromatography (GPC).

2.3. Synthesis of GO and NGO-PEG

GO was synthesized with natural graphite flake using a modified Hummer's method as reported elsewhere [2,19]. To prepare NGO, exfoliation was carried out by sonicating 1.0 mg/mL of GO suspension for 4 h with a small tip of Branson sonifier (Fisher, Pittsburgh, PA) in a refrigerated circulator (Jeio Tech, Korea). After that, 10 mL of 2.0 mg/mL NGO suspension was mixed with chloroacetic acid (1.0 g) and NaOH (1.2 g), which resulted in carboxylic acid functionalized NGO. The resulting NGO–COOH was neutralized, and purified by repeated rinsing and filtration. PEG-amine (2.0 kDa) was added to the NGO–COOH suspension both at a final concentration of 1.0 mg/mL and sonicated in a bath sonicator for 5 min. NGO-PEG was prepared by the addition of EDC (5.0 mM), which was sonicated for 30 min and finally stirred at room temperature for 12 h. The reaction was quenched with mercaptoethanol and the final product was dialyzed against deionized water for 24 h. The prepared samples were characterized by Fourier transform – infrared spectroscopy (FT-IR, Thermo Nicolet, Madison, WI), UV–visible spectroscopy (Thermo Evolution Array, Madison, WI), transmission electron microscopy (TEM, Phillips CM200, Madison, WI), and atomic force microscopy (AFM, Veeco Multimode Scanning Probe Microscope with the NanoScope IV Controller, Santa Barbara, CA).

2.4. Assessment of fluorescence quenching and recovery

The concentration of f-DEVD was estimated by measuring the concentration of ssDNA in the f-DEVD-ssDNA conjugate using NanoDrop N-1000 (Thermo, Madison, WI). One unit of the absorbance at 260 nm corresponded to *ca.* 33 μg of f-DEVD. To the 10 μL of aliquot of the probe solution containing 10 ng of the probe, 90 μL of predetermined amount of NGO-PEG conjugate in PBS was added with mild stirring. After incubation at room temperature for 6 h, the residual fluorescence signal intensity in the region of interest (ROI) was recorded as photons per sec per square centimeter per steradian (p/sec/cm^2/sr) and analyzed with a fluorescence imaging system (Xenogen, Almeda, CA). The f-DEVD-ssDNA/NGO-PEG complex was also characterized by AFM and UV–visible spectroscopy. Then, the specific fluorescence recovery by capasae-3 was assessed with the f-DEVD-ssDNA/NGO-PEG complex formulated at a weight ratio of 79/21 as described above. An aliquot of the resulting complex (20 μL, 2 ng probe) was slowly added to 80 μL of the PBS containing various amounts of recombinant human caspase-3. After incubation for 30 min, fluorophotometric analysis was carried out with a Fluoroskan Ascent FL microplate fluorometer (Thermo, Madison, WI) at the excitation/emission wavelength of 540/575 nm.

2.5. Monitoring of intracellular caspase-3 by confocal microscopy

A549 cells were cultivated at a density of 2×10^4 cells/well on a 4 well chamber slide (LAB-TEK, Naperville, IL) for 24 h and treated with 100 μL of the prepared complex solution in PBS containing *ca.* 10 ng/mL of f-DEVD at 37 °C for 1 h. After washing with PBS thrice, the cells were incubated with 1.8 μg/mL of STS or 300 μg/mL of TRAIL for 3 h and stained with DAPI (1.5 μg/mL) in PBS for 10 min. Then, TUNEL staining was performed as described in the manufacturer's protocol (Roche Applied Science, Mannheim, Germany) to monitor the cell apoptosis with a LSM510 confocal laser scanning microscope (Carl Zeiss, Oberkochen, Germany). In order for colorimetric assay of caspase-3 activity in live cells, A549 cells were cultured on a 96 well culture plate at a density of 5×10^4 cells per well for 24 h and treated with 10 μL of the prepared complex solution in PBS containing 10 ng/mL of the probe. After washing with PBS thrice, the cells were incubated with a different amount of TRAIL at room temperature for 6 h. The residual fluorescence signal intensity in the ROI was recorded as photons per sec per square centimeter per steradian (p/sec/cm^2/sr) and analyzed with a fluorescence imaging system (Xenogen, Almeda, CA). As a control experiment, cells were pre-incubated with various concentrations of capase-3 inhibitor of Z-DEVD-FMK and assessed as described above.

2.6. Induction of cerebral hypoxic-ischemia and the bioimaging

Sprague Dawley (SD) rat pups (7 days old, Daihan Biolink Co., Seoul, Korea) were anesthetized in a small box with isoflurane and a surgical procedure for right common carotid-artery ligation was performed under isoflurane anesthesia within 3 min. Upon recovery from anesthesia, the rat pups were returned to their natural dams. After stabilization for 2 h post-surgery, the animals were exposed to hypoxia (8% O_2 and 92% N_2) at 37 °C for 2 h. Pups in the normoxia control group received a sham operation without carotid-artery ligation. After hypoxic-ischemia for 24, 36, and 48 h, they were anesthetized with pentobarbital (60 mg/kg, intraperitoneally) and then treated by the injection of 5 μL of f-DEVD-ssDNA/NGO-PEG complex containing 0.5 ng of the probe through a 31-gauge syringe into both hemispheres with the following stereotactic guidance (Digital Stereotaxic Instrument w/Fine Drive, St. Louis, MO): coordinates, $x = \pm 0.5$, $y = +1.0$, $z = +2.0$ mm relative to the bregma. Thirty min post-injection, animals were anesthetized and perfused intracardially with PBS (pH 7.4), and the skull and meninges were carefully removed for the fluorescent bioimaging. Then, the harvested brain was transected in the coronal plane into two portions at the bregma level. The anterior portion of the brain was processed for triphenyltetrazolium chloride (TTC) staining. The posterior portion of the brain was post-fixed in 4% formaldehyde and processed for hematoxylin and eosin (H&E), TUNEL, and toluidine blue (TB) staining, as well as TEM and confocal microscopic imaging. The bioimaging experiments for hypoxic-ischemic encephalopathy (HIE) were performed three times. The animals were treated in accordance with guidelines set forth by the American Association for the Accreditation of Laboratory Animal Care (AAALAC), and all studies with rats were reviewed and approved by the Institutional Animal Care and Use Committee of Samsung Biomedical Research Institute.

2.7. Induction of liver damage and the bioimaging

SD rats with a mean body weight of *ca.* 600 g were used for the bioimaging with f-DEVD-ssDNA/NGO-PEG complex in the liver disease models. A total of 8 animals were divided into four groups ($n = 2$): A control group with intraperitoneal (*ip*) injections of saline, and three liver disease model groups with *ip* daily injections of N-nitrosodimethylamine (NDMA) at a dose of 4, 5 or 10 mg/(kg body weight) for five consecutive days, respectively. After 9 days, the animals were treated by intravenous (*iv*) injection of f-DEVD-ssDNA/NGO-PEG complex containing 50 ng of the probe. Thirty min post-injection of the complex, the animals were sacrificed by decapitation, and three different organs of liver, spleen and kidney were harvested for the NIRF imaging analysis.

2.8. Statistical analysis

All experiments were replicated more than three times and the resulting data were statistically analyzed by ANOVA tests using a commercially available software of GraphPad Prism (GraphPad, La Jolla, CA).

3. Results and discussion

3.1. Synthesis and characterization of fluorescent capase-3 specific probe and NGO-PEG

As schematically shown in Fig. 1a, PEGylated NGO makes a stable complex with 18-nucleotide partial sequences of *E. coli* RNA

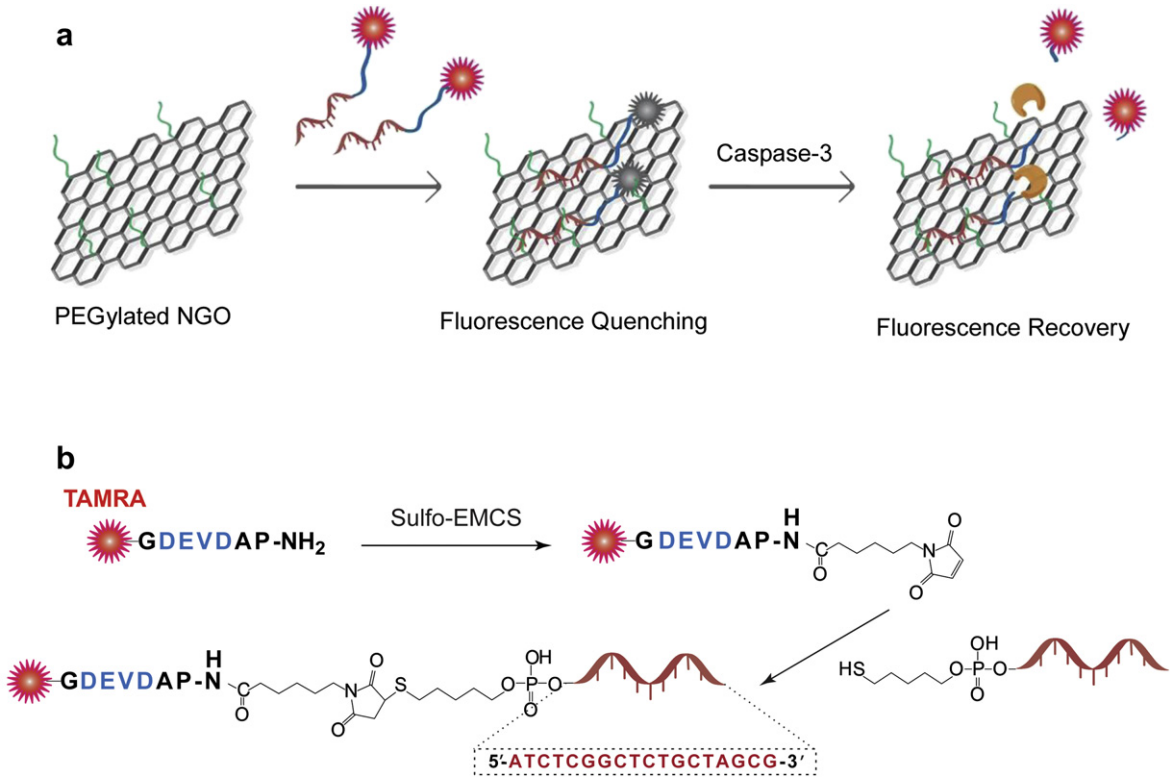

Fig. 1. a) Schematic illustration of fluorescent TAMRA-DEVD-ssDNA/NGO-PEG complex for the monitoring of intracellular caspase-3 protease activity *in vitro* and *in vivo*. (b) Synthetic scheme of the TAMRA-DEVD-ssDNA conjugate.

I which is conjugated to TAMRA labeled caspase-3 specific peptide substrate of f–NH_2–DEVD. The complex formation by π-π stacking results in the fluorescence quenching by FRET. *E. coli* RNA I is involved in the replication of ColE1-type plasmid in *E. coli*. Because mammalian cells do not have a complementary nucleic acid to the sequence of RNA I oligo-DNA, the ssDNA does not hybridize with complementary sequences nor displace it from the NGO surface during its diagnostic applications [27]. At the same time, ssDNA anchor might be protected from enzymatic attack by the complex formation with NGO [28]. The probe peptide – ssDNA conjugate was prepared by the coupling reaction of f–NH_2–DEVD and sulfhydryl group at 5′-end of ssDNA using a bifunctional linker of sulfo-EMCS (Fig. 1b). The resulting f-DEVD-ssDNA conjugate was characterized by agarose gel electrophoresis and GPC. After staining with ethidium bromide, the f–DEVD peptide exhibited a mobility toward (+) direction and formed a clear band confirming the successful conjugation of the peptide to negatively charged ssDNA (Fig. S1). With the band migration, color change from red to orange color was observed, which might be attributed to the co-localization of ethidium bromide and TAMRA. The retention time of the major peak on the GPC chromatogram corresponding to the DNA was shifted revealing the successful conjugation of ssDNA with f–DEVD peptide (Fig. S2).

In order to prepare NGO-PEG, GO was first synthesized with graphite powder by using a modified Hummer's method [2,19]. TEM of GO samples showed the characteristic translucent sheets of GO with wrinkles and folds in a lateral dimension of micrometer scale (Fig. S3). NGO was prepared with the GO flakes by intensive sonication in a bath circulator equipped with a refrigerator. FT–IR of NGO samples showed the characteristic aromatic C=C bonds and C=O stretch at the wavelength of 1700 cm^{-1} and 1580 cm^{-1}, respectively (Fig. S4). AFM images showed the well dispersed morphology of NGO flakes with a lateral width of less than 150 nm and a topological height of less than 1 nm (Fig. 2). Then, the NGO was activated with chloroacetic acid in a strong basic condition to introduce carboxyl groups on NGO (NGO–COOH), which was further modified with PEG-amine by amide bond formation using EDC. FT–IR showed the characteristic peak of carboxyl group at 1630 cm^{-1}, and those of $-CH_2-$ and –CO–NH- at 2860 cm^{-1} and 1650 cm^{-1}, respectively (Fig. S4). In addition, the morphology of NGO–COOH and NGO-PEG was assessed by AFM. The topological height of NGO–COOH and NGO-PEG slightly increased from *ca.* 1.0 nm–1.2 nm and 2.3 nm (Fig. 2), which might be attributed to the carboxyl modification and the PEGylation. From the results, we could confirm the successful preparation of NGO-PEG.

3.2. Preparation and characterization of self-assembled f-DEVD–ssDNA/NGO-PEG complex

We prepared and characterized the noncovalent complex of the florescent probe and NGO-PEG by π-π stacking. When the predetermined amount of f-DEVD-ssDNA (100 ng/mL) was mixed with NGO-PEG at various concentrations up to 79.2 μg/mL in PBS (pH = 7.4), the fluorescence of f-DEVD-ssDNA gradually decreased in an NGO concentration-dependent manner due to the fluorescence quenching by FRET with increasing formation of f-DEVD-ssDNA/NGO-PEG complex (Fig. 3a). The quenching did not evolve significantly at an NGO-PEG concentration higher than 79.2 μg/mL. The f-DEVD-ssDNA/NGO-PEG complex exhibited a big increase in the topological height from *ca.* 2.3 nm–4.3 nm, when compared with bare NGO-PEG (Fig. 2). The hydrodynamic diameter of the complexes also slightly increased from *ca.* 78 nm–92 nm in comparison with NGO-PEG (Fig. S5a). In addition, the zeta potential of TAMRA-DEVD-ssDNA/NGO-PEG complex slightly decreased in

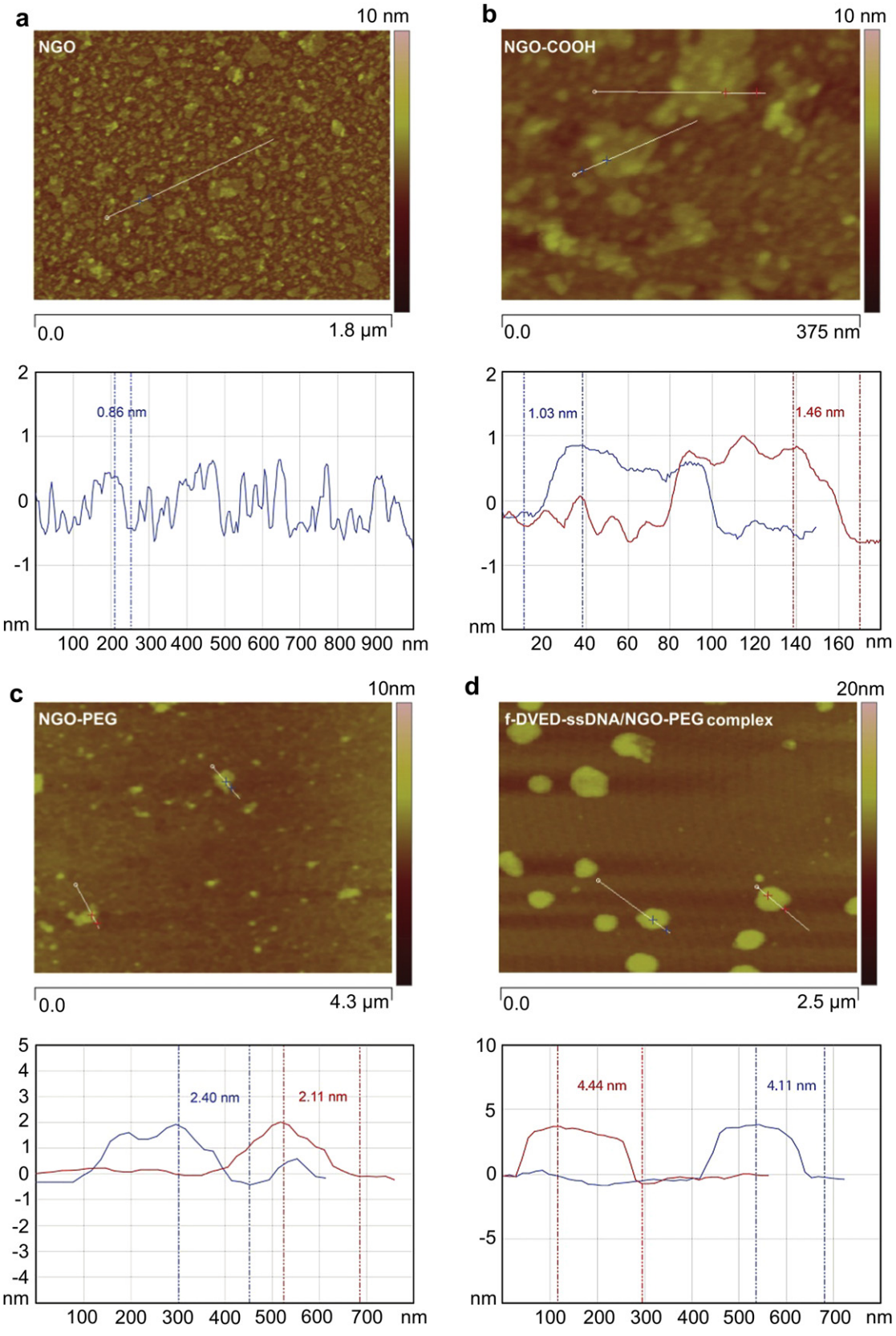

Fig. 2. AFM height profiles of (a) NGO, (b) NGO-COOH, (c) NGO-PEG, and (d) TAMRA-DEVD-ssDNA/NGO-PEG complex.

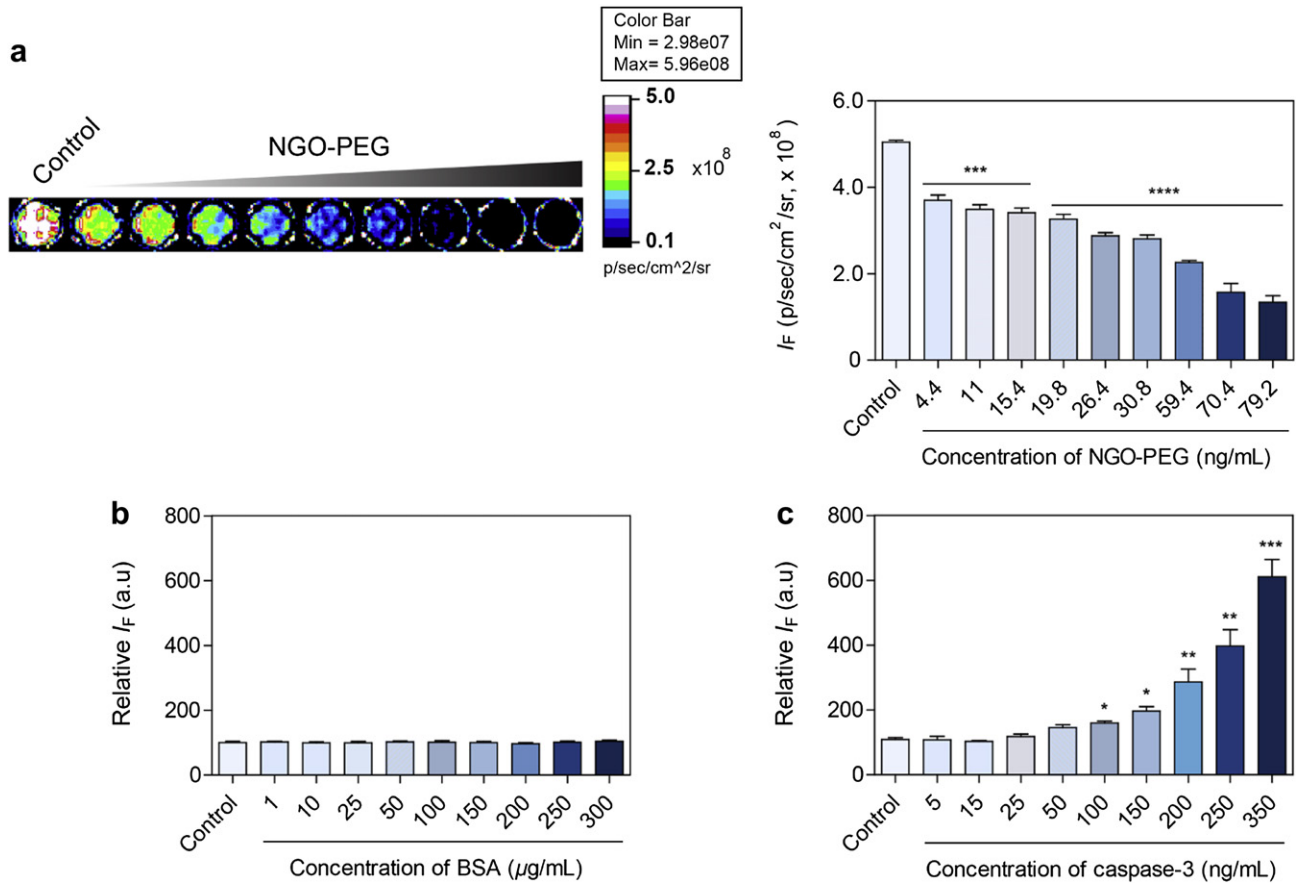

Fig. 3. a) NIRF image of microplate containing TAMRA-DEVD-ssDNA conjugate after incubation with various concentrations of NGO-PEG. The quenched fluorescence intensity was quantified in the rectangular region of interest (ROI). (b) The relative NIRF intensity after incubation with various concentrations of BSA for 1 h. (c) The relative NIRF intensity after incubation with various concentrations of recombinant human capase-3 for 1 h ($n = 8$, $^*P < 0.05$, $^{**}P < 0.01$, $^{***}P < 0.001$, $^{****}P < 0.0001$).

comparison with that of NGO-PEG reflecting the binding of negatively charged ssDNA to the surface of NGO-PEG (Fig. S5b). As a representative protein in the serum, BSA did not cause any significant increase of fluorescence intensity after incubation up to a concentration of 300 μg/mL for 1 h (Fig. 3b) confirming the serum stability of the complex for diagnostic applications. To verify the specific cleavage and the following fluorescence recovery of f-DEVD-ssDNA/NGO-PEG complex by active caspase-3 during apoptosis, the complex at an f-DEVD-ssDNA concentration of 100 ng/mL was incubated with increasing concentrations of recombinant human caspase-3 for 1 h. The f-DEVD-ssDNA/NGO-PEG complex showed a gradual and significant increase in fluorescence intensity with increasing concentration of caspase-3 up to 350 ng/mL (Fig. 3c).

3.3. Monitoring of intracellular caspase-3 by confocal microscopy and fluorophotometry

The f-DEVD-ssDNA/NGO-PEG complex at a weight ratio of 79/21 was exploited for real-time monitoring of caspase-3 protease activity in live A549 cells. The prepared complexes were taken up to A549 cells within 1 h and then apoptosis was induced by the treatment with STS (1.8 μg/mL) or TRAIL (300 ng/mL). During incubation with the apoptosis inducer of STS for 3 h, the morphology of the cells was changed and the formation of apoptotic-bodies was clearly observed by optical microscopy (Fig. S6). While the control cells without apoptosis inducer treatment did not show any detectable NIRF signals, the cells treated with STS or TRAIL exhibited fluorescent signals on the confocal microscopic images (Fig. S6c and 4). The signals were thought to result from the cleavage of fluorescent substrate peptide immobilized on the surface of NGO-PEG by caspase-3. The DNA fragmentation also represents a characteristic hallmark of apoptosis. It is well known that activated caspase-3 translocates from cytoplasm into nucleus and initiates apoptotic DNA fragmentation. As shown in Fig. 4, TUNEL staining revealed a good co-localization together with the NIRF signals in the nucleus.

As a colorimetric assay system, the dose dependent response of TRAIL was monitored in a multiwell plate with the f-DEVD-ssDNA/NGO-PEG complex. With increasing concentration of TRAIL from 50 to 300 ng/mL, the fluorescence intensity was enhanced in the cells treated with f-DEVD-ssDNA/NGO-PEG complex (Fig. 5a). Furthermore, the effect of caspase-3 inhibitor of Z-DEVD-FMK on intracellular fluorescence activation was also investigated with the same procedures (Fig. 5b). NIRF signals were significantly reduced upon exposure to the caspase-3 inhibitor before the treatment with TRAIL, which was in good agreement with the previous report [19]. The f–DEVD–ssDNA/NGO-PEG complex was cytocompatible in A549 cells with increasing concentration of NGO-PEG up to 100 μg/mL (Fig. S7). From the results, we could confirm that the non-covalent f–DEVD–ssDNA/NGO-PEG complex effectively detected the caspase-3 activation during the progress of apoptosis in live cells.

3.4. Bioimaging of cerebral hypoxic-ischemia and liver cirrhosis

The f–DEVD–ssDNA/NGO-PEG complex was applied to *in vivo* diagnosis of hypoxic-ischemic encephalopathy (HIE) as a model

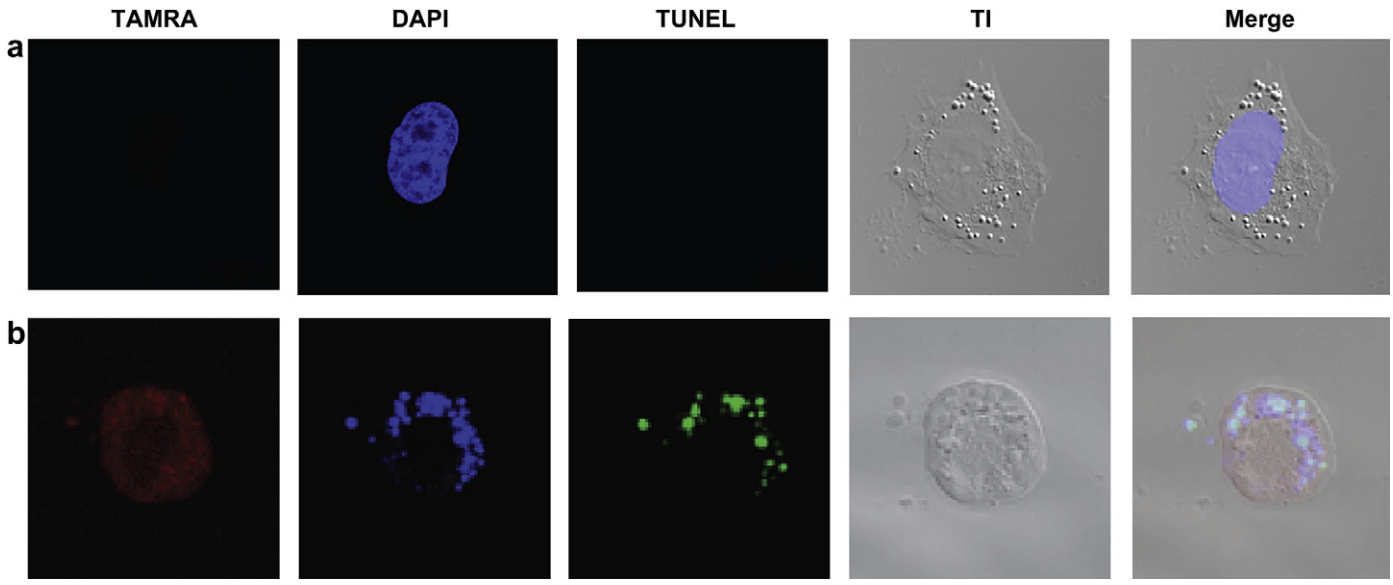

Fig. 4. Confocal microscopic images of A549 cells after incubation with TAMRA-DEVD-ssDNA/NGO-PEG complex for 1 h, followed by the treatment with (a) PBS and (b) TRAIL for 3 h (TAMRA: fluorescence image of TAMRA, DAPI: fluorescence image after DAPI staining, TUNEL: fluorescence image after TUNEL staining, TI: transmitted light image, and Merge: confocal image merged with transmitted light image).

system of apoptosis-related diseases using 7 days old SD rat pups. The HIE model was prepared by carotid-artery ligation, which exacerbates neuronal apoptosis and gradually enhances temporal distribution of caspase-3 in the brain [29]. The ischemic time dependent brain injury could be correlated with the fluorescence signal intensity by NIRF imaging after injection of the f–DEVD–ssDNA/NGO-PEG complex (Fig. 6a). Then, the brain tissues were cryo-sectioned to analyze the apoptosis in a cellular level. Fig. 6b shows representative confocal microscopic images of the non-infarcted and infarcted hemispheres 30 min after injection of the f–DEVD–ssDNA/NGO-PEG complex. In case of the non-infarcted hemisphere, cells were arranged concretely in extracellular matrix (ECM) and did not show the fluorescence of TAMRA. In contrast, the cells in the infarcted hemisphere were arranged roughly in destroyed ECM showing the fluorescence of TAMRA (Fig. 6b). TTC and H&E staining confirmed that the fluorescent site of f–DEVD–ssDNA/NGO-PEG complex was identical to the site of HIE (Fig. 7a). After TUNEL and TB staining, and TEM imaging, photomicrographs of the brain treated by the carotid-artery ligation also confirmed the occurrence of hypoxic-ischemic damage and the consequent apoptosis in the brain (Fig. 7b). Moreover, the systemically delivered f–DEVD–ssDNA/NGO-PEG complex could

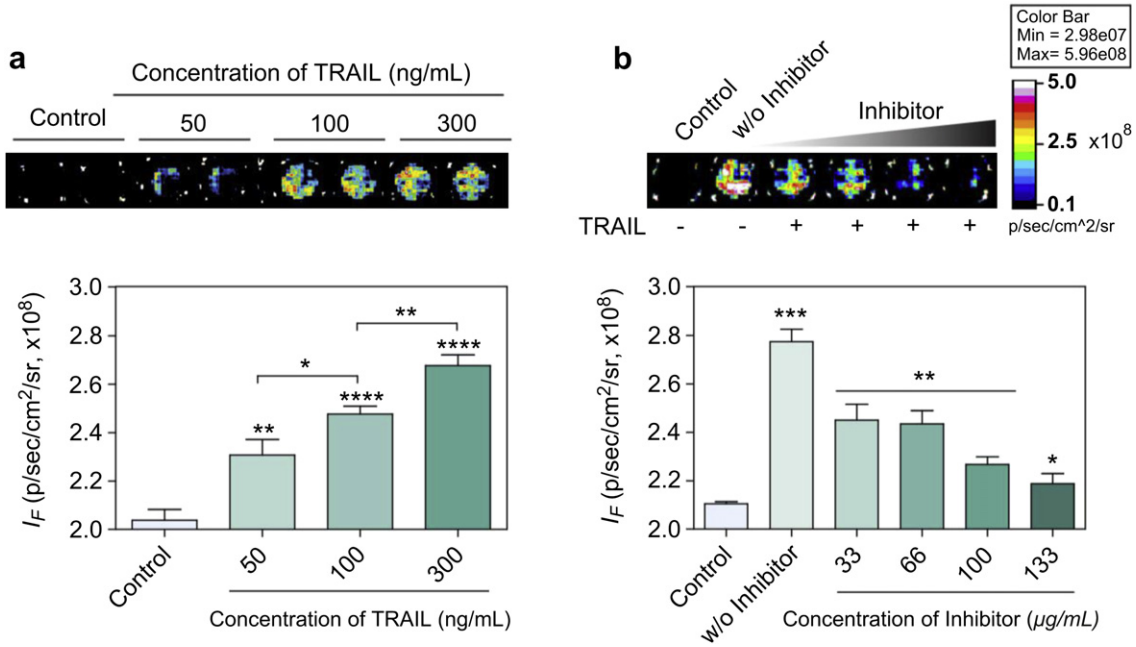

Fig. 5. NIRF images and the fluorescence intensity values of the rectangular ROI in micro-plates after incubation of A549 cells with TAMRA-DEVD-ssDNA/NGO-PEG complex for 1 h, followed by the treatment with increasing concentration of TRAIL for 3 h (a) In the absence and (b) In the presence of a different concentration of caspase-3 inhibitor (Z-DEVD-FMK) ($n = 8$, $^{*}P < 0.05$, $^{**}P < 0.01$, $^{***}P < 0.001$, $^{****}P < 0.0001$).

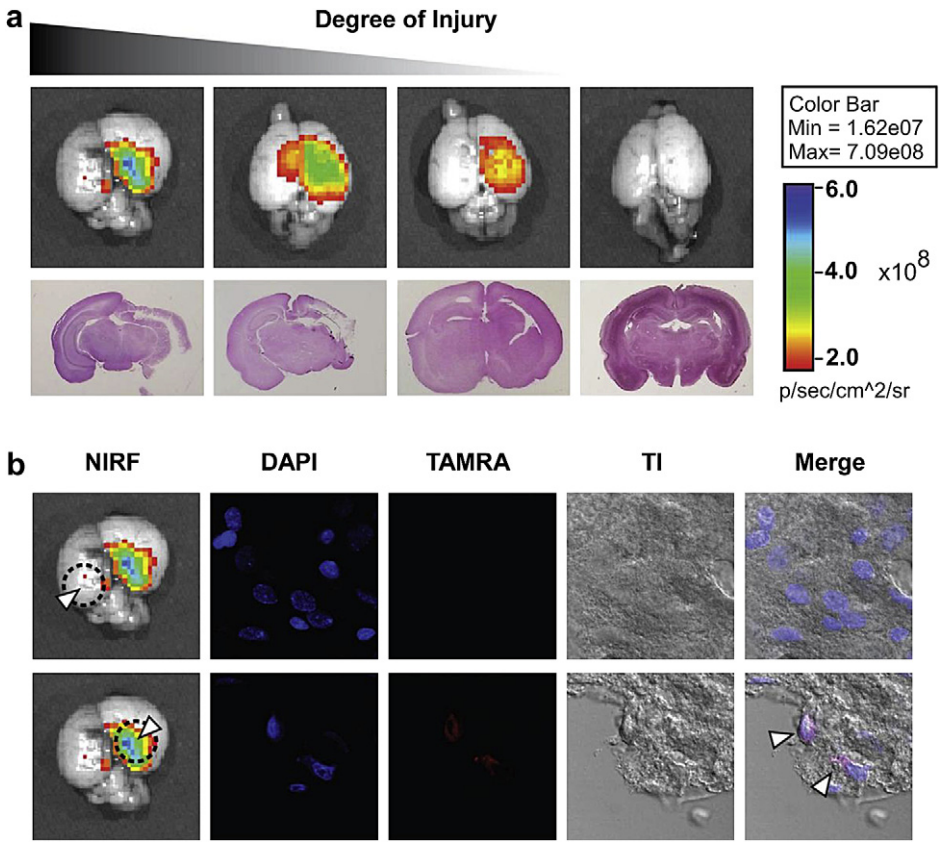

Fig. 6. a) NIRF and the corresponding H&E staining images of apoptotically damaged brains with a different degree of hypoxic-ischemia after injection of TAMRA-DEVD-ssDNA/NGO-PEG complex. From right to the left, the hypoxic-ischemic brain images by carotid-artery ligation for 0, 24, 36, and 48 h. (b) Representative confocal microscopic images of the non-infarcted and infarcted hemispheres after treatment by the injection of TAMRA-DEVD-ssDNA/NGO-PEG complex for 30 min.

visualize the degree of apoptotic liver damage in SD rats by the treatment with NDMA for 5 days (Fig. 8). The NIRF images of harvested liver samples clearly showed the NDMA concentration dependent gradual increase in the fluorescent signal intensity. The fluorescence intensity was also slightly increased in kidney samples, which might be attributed to the renal extravasation of enzymatically cleaved fragment of peptide substrate. From the results, the self-assembled NGO complex was thought to be successfully applied to the molecular diagnosis of HIE in neonatal rats and liver cirrhosis in SD rats for the first time reflecting the

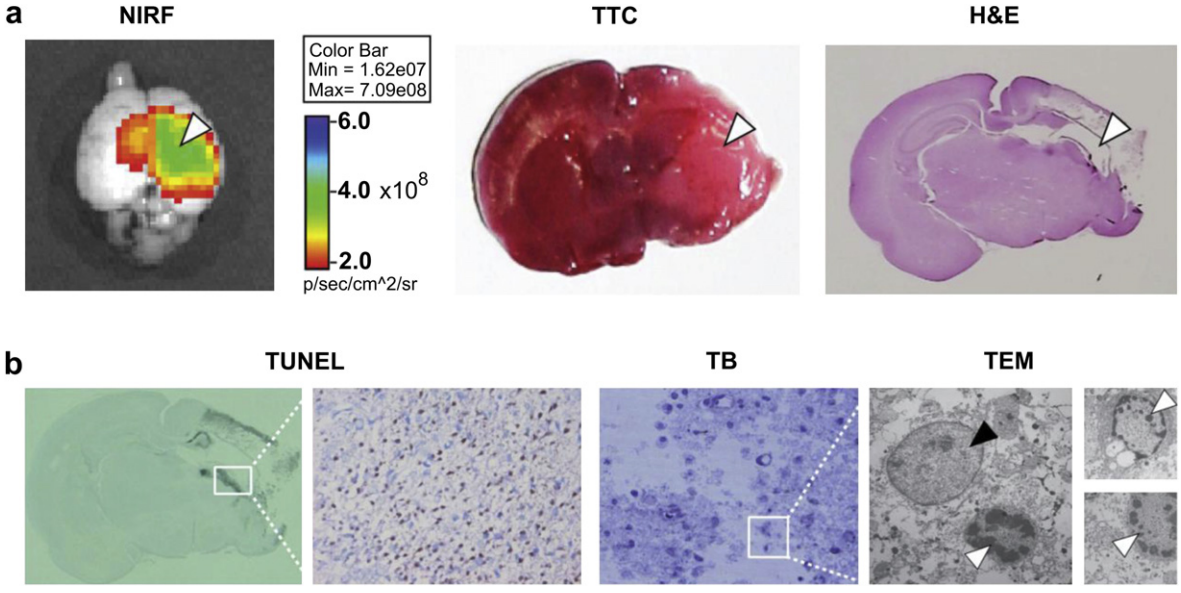

Fig. 7. a) Representative NIRF image, and photomicrographs of the hypoxic-ischemic brain after triphenyltetrazolium chloride (TTC) staining and H&E staining. The white arrow heads indicate the area of infarction. (b) Photomicrographs of hypoxic-ischemic brain after TUNEL staining and Toluidine Blue (TB) staining, and the corresponding TEM images. The black arrow head indicates brain cells undergoing cell death by necrosis and the white arrow heads indicate brain cells undergoing cell death by apoptosis. (For interpretation of the references to colour in this figure legend, the reader is referred to the web).

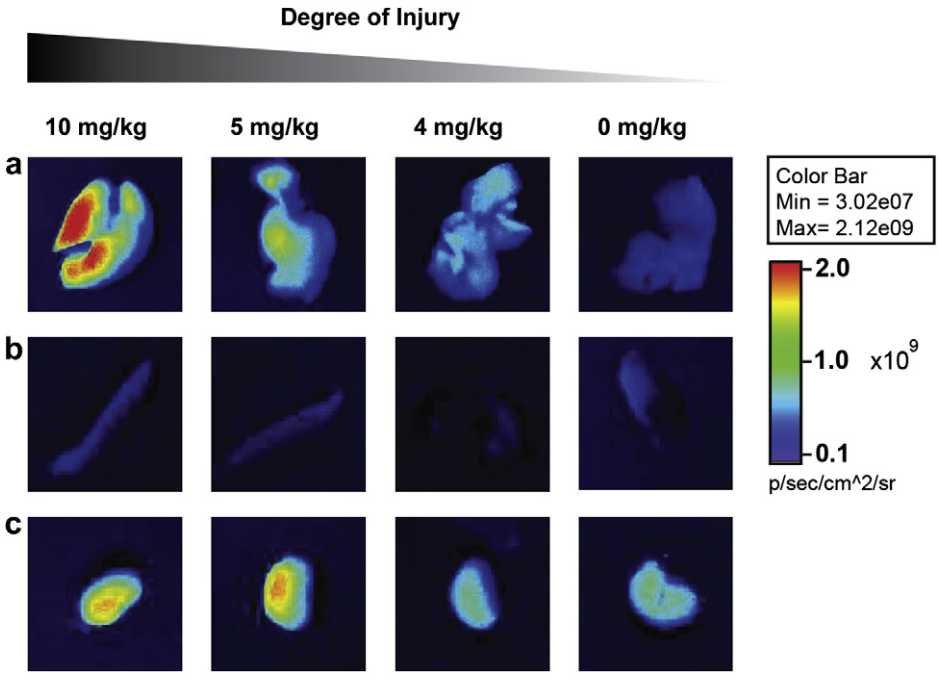

Fig. 8. NIRF images of (a) liver, (b) spleen, and (c) kidney harvested from apoptotic liver disease model SD rats after *iv* injection of TAMRA-DEVD-ssDNA/NGO-PEG complex. The liver disease models from right to left were prepared by daily *ip* injection of 0, 4, 5, 10 (mg NDMA)/(kg body weight) for five consecutive days.

feasibility for the facile diagnosis of apoptosis-related diseases like neurodegenerative diseases, inflammatory diseases, cancer, hematologic diseases, and autoimmune diseases. The multiplex diagnostic systems by multiple stacking of cleavable fluorescent probe peptides-ssDNA conjugates on the NGO-PEG might simultaneously detect various kinds of biomarkers contributing to the more accurate diagnosis of apoptotic diseases. With efficient drug loading on the graphitic domain, the NGO complex can be also exploited as a theranostic system for a diagnostic therapy.

4. Conclusions

We successfully developed the non-covalent TAMRA-DEVD-ssDNA/NGO-PEG complex as a simple, rapid, and efficient platform for real-time imaging and monitoring of caspase-3 activation during the progress of apoptosis *in vitro* and *in vivo*. The NIRF TAMRA labeled capase-3 cleavable peptide substrate of TAMRA-DEVD was conjugated to a partial sequence of *E. coli* RNAI, which was self-assembled for the complex formation with NGO-PEG via π-π stacking. The self-assembled NGO complex made possible the monitoring the caspase-3 activity in live A549 cells, and the molecular diagnosis of hypoxic-ischemic encephalopathy in neonatal SD rats and liver damage in SD rats. From the results, we could confirm the feasibility of the NGO complex for caspase-specific bioimaging and the diagnosis of various apoptosis-related diseases.

Acknowledgment

This work was financially supported by the Converging Research Center Program through the National Research Foundation of Korea (NRF) funded by the Ministry of Education, Science and Technology (2009-0081871). This work was also financially supported by POSCO (#4.0007652.09). This study was also supported by Mid-career Researcher Program through NRF grant funded by the MEST (No. 2009-0084578).

Appendix A. Supplementary data

Supplementary data related to this article can be found online at http://dx.doi.org/10.1016/j.biomaterials.2012.06.086.

References

[1] Kim YS, Rutka JT, Chan WCW. Nanomedicine. New Engl J Med 2010;363:2434–43.
[2] Noorden R. The trials of new carbon. Nature 2011;469:14–6.
[3] Ling Y, Pong T, Vassiliou CC, Huang PL, Cima MJ. Implantable magnetic relaxation sensors measure cumulative exposure to cardiac biomarkers. Nat Biotechnol 2011;29:273–7.
[4] An TC, Kim KS, Hahn SK, Lim GB. Real-time, step-wise, electrical detection of protein molecules using dielectrophoretically aligned SWNT-film FET aptasensors. Lab on a Chip 2010;10:2052–6.
[5] Kim KS, Lee HS, Yang JA, Jo MH, Hahn SK. The fabrication, characterization and application of aptamer-functionalized Si-nanowire FET biosensors. Nanotechnology 2009;20:235501.
[6] Artiles MS, Rout CS, Fisher TS. Graphene-based hybrid materials and devices for biosensing. Adv Drug Deliv Rev 2011;63:1352–60.
[7] Yang W, Ratinac KR, Ringer SR, Thordarson P, Gooding JJ, Braet F. Carbon nanomaterials in biosensors: should you use nanotubes or graphene. Angew Chem Int Ed 2010;49:2114–38.
[8] He SJ, Song B, Li D, Zhu CF, Qi WP, Wen YQ, et al. A graphene nanoprobe for rapid, sensitive, and multicolor fluorescent DNA analysis. Adv Funct Mater 2010;20:453–9.
[9] Zhang M, Yin BC, Wang XF, Ye BC. Interaction of peptides with graphene oxide and its application for real-time monitoring of protease activity. Chem Commun 2011;47:2399–401.
[10] Bao H, Pan Y, Ping Y, Sahoo NG, Wu T, Li L, et al. Chitosan-functionalized graphene oxide as a nanocarrier for drug and gene delivery. Small 2011;7:1569–78.
[11] Zhang L, Xia J, Zhao Q, Liu L, Zhang Z. Functional graphene oxide as a nanocarrier for controlled loading and targeted delivery of mixed anticancer drugs. Small 2010;6:537–44.
[12] Swathi RS, Sebastian KL. Long range resonance energy transfer from a dye molecule to graphene has (distance)(−4) dependence. J Chem Phys 2008;129:086101.
[13] Yang K, Zhang S, Zhang GX, Sun XM, Lee ST, Liu Z. Graphene in mice: ultrahigh in vivo tumor uptake and efficient photothermal therapy. Nano Lett 2010;10:3318–23.
[14] Liu F, Choi JY, Seo TS. Graphene oxide arrays for detecting specific DNA hybridization by fluorescence resonance energy transfer. Biosens Bioelectron 2010;25:2361–5.

[15] Chang HX, Tang LH, Wang Y, Jiang J, Li J. Graphene fluorescence resonance energy transfer aptasensor for the thrombin detection. Anal Chem 2010;82:2341–6.
[16] Jung JH, Cheon DS, Liu F, Lee KB, Seo TS. A graphene oxide based immunobiosensor for pathogen detection. Angew Chem Int Ed 2010;49:5708–11.
[17] Huang PJJ, Kempaiah R, Liu J. Synergistic pH effect for reversible shuttling aptamer-based biosensors between graphene oxide and target molecules. J Mater Chem 2011;21:8991–3.
[18] Friedlander RM. Apoptosis and caspases in neurodegenerative diseases. N Engl J Med 2003;348:1365–75.
[19] Wang H, Zhang Q, Chu X, Chen T, Ge J, Yu R. Graphene oxide - peptide conjugate as an intracellular protease sensor for caspase-3 activation imaging in live cell. Angew Chem Int Ed 2011;50:7065–9.
[20] Eltzschig HK, Eckle T. Ischemia and reperfusion - from mechanism to translation. Nat Med 2011;17:1391–401.
[21] Enari M, Sakahira H, Yokoyama H, Okawa K, Iwamatsu A, Nagata S. A caspase-activated DNase that degrades DNA during apoptosis, and its inhibitor ICAD. Nature 1998;391:43–50.
[22] Huang Q, Li F, Liu X, Li W, Shi W, Liu FF, et al. Caspase 3-mediated stimulation of tumor cell repopulation during cancer radiotherapy. Nat Med 2011;17:860–6.
[23] Sun IC, Lee S, Koo H, Kwon IC, Choi K, Ahn CH, et al. Caspase sensitive gold nanoparticle for apoptosis imaging in live cells. Bioconjug Chem 2010;21:1939–42.
[24] Lin SY, Chen NT, Sun SP, Chang JC, Wang YC, Yang CS, et al. The protease-mediated nucleus shuttles of subnanometer gold quantum dots for real-time monitoring of apoptotic cell death. J Am Chem Soc 2010;132:8309–15.
[25] Jun YW, Sheikholeslami S, Hostetter DR, Tajon C, Craik CS, Alivisatos AP. Continuous imaging of plasmon rulers in live cells reveals early-stage caspase-3 activation at the single-molecule level. Proc Natl Acad Sci USA 2009;106:17735–40.
[26] Kim K, Lee M, Park H, Kim JH, Kim S, Chung H, et al. Cell-permeable and biocompatible polymeric nanoparticles for apoptosis imaging. J Am Chem Soc 2006;128:3490–1.
[27] Kim JH, Jang HH, Ryou SM, Kim S, Bae J, Lee K, et al. A functionalized gold nanoparticles-assisted universal carrier for antisense DNA. Chem Commun 2010;46:4151–3.
[28] Lu CH, Zhu CL, Li J, Liu JJ, Chen X, Yang HH. Using graphene to protect DNA from cleavage during cellular delivery. Chem Commun 2010;46:3116–8.
[29] Nakajima W, Ishida A, Lange MS, Gabrielson KL, Wilson MA, Martin LJ, et al. Apoptosis has a prolonged role in the neurodegeneration after hypoxic ischemia in the newborn rat. J Neurosci 2000;20:7994–8004.